Atmos. Chem. Phys., 13, 1011–1022, 2013
www.atmos-chem-phys.net/13/1011/2013/
doi:10.5194/acp-13-1011-2013

Atmospheric Chemistry and Physics

Effect of aerosols and NO_2 concentration on ultraviolet actinic flux near Mexico City during MILAGRO: measurements and model calculations

G. G. Palancar[1,2], B. L. Lefer[3], S. R. Hall[1], W. J. Shaw[4], C. A. Corr[5], S. C. Herndon[6], J. R. Slusser[7], and S. Madronich[1]

[1]Atmospheric Chemistry Division, National Center for Atmospheric Research, Boulder, CO, USA
[2]INFIQC-CONICET, Departamento de Físico Química, Facultad de Ciencias Químicas, Universidad Nacional de Córdoba, Centro Láser de Ciencias Moleculares, 5000, Córdoba, Argentina
[3]Department of Earth and Atmospheric Sciences, University of Houston, Houston, TX, USA
[4]Pacific Northwest National Laboratory, Department of Energy, Richland, WA, USA
[5]Earth Systems Research Center, University of New Hampshire, Durham, NH, USA
[6]Aerodyne Research Inc., Billerica, MA, USA
[7]UV-B Monitoring and Research Program, USDA, Colorado State University, Ft. Collins, CO, USA

Correspondence to: S. Madronich (sasha@ucar.edu)

Received: 25 June 2012 – Published in Atmos. Chem. Phys. Discuss.: 3 August 2012
Revised: 24 December 2012 – Accepted: 13 January 2013 – Published: 24 January 2013

Abstract. Urban air pollution absorbs and scatters solar ultraviolet (UV) radiation, and thus has a potentially large effect on tropospheric photochemical rates. We present the first detailed comparison between actinic fluxes (AF) in the wavelength range 330–420 nm measured in highly polluted conditions and simulated with the Tropospheric Ultraviolet-Visible (TUV) model. Measurements were made during the MILAGRO campaign near Mexico City in March 2006, at a ground-based station near Mexico City (the T1 supersite) and from the NSF/NCAR C-130 aircraft. At the surface, measured AF values are typically smaller than the model by up to 25 % in the morning, 10 % at noon, and 40 % in the afternoon, for pollution-free and cloud-free conditions. When measurements of PBL height, NO_2 concentration and aerosols optical properties are included in the model, the agreement improves to within ±10 % in the morning and afternoon, and ±3 % at noon. Based on daily averages, aerosols account for 68 % and NO_2 for 25 % of AF reductions observed at the surface. Several overpasses from the C-130 aircraft provided the opportunity to examine the AF perturbations aloft, and also show better agreement with the model when aerosol and NO_2 effects are included above and below the flight altitude. TUV model simulations show that the vertical structure of the actinic flux is sensitive to the choice of the aerosol single scattering albedo (SSA) at UV wavelengths. Typically, aerosols enhance AF above the PBL and reduce AF near the surface. However, for highly scattering aerosols (SSA > 0.95), enhancements can penetrate well into the PBL, while for strongly absorbing aerosols (SSA < 0.6) reductions in AF are computed in the free troposphere as well as in the PBL. Additional measurements of the SSA at these wavelengths are needed to better constrain the effect of aerosols on the vertical structure of the AF.

1 Introduction

Urban and regional photochemical smog is reasonably well understood as a byproduct of reactions between volatile organic compounds (VOCs) and nitrogen oxides (NO_x) under solar ultraviolet (UV) radiation (Haagen-Smit et al., 1953; Finlayson Pitts and Pitts, 1999). Changes in emissions of VOCs and NO_x affect both the timing and intensity of smog episodes, with specific responses depending on whether the chemical regime is NO_x-limited, VOC-limited, or NO_x-inhibited (Dimitriades, 1972; Sillman, 1999;

Kleinman, 2005; Stephens et al., 2008). Regardless of the VOC-NO_x regime, smog chemistry is photon-limited and therefore always sensitive to changes in the UV radiation field. In polluted regions these radiation changes can be caused by the products of smog chemistry, especially ozone (O_3), nitrogen dioxide (NO_2), and aerosol particles. Thus an interesting feedback exists by which photochemical smog production depends on the UV radiation, but can also modify it. Whether the net effect is an increase or decrease in photochemistry depends on the relative importance of scattering and absorption by these secondary pollutants and their vertical distributions. Solar photons ($h\nu$) initiate and sustain smog photochemistry by breaking relatively stable molecules into much more reactive fragments, i.e. the photolysis of nitrogen dioxide (NO_2)

$$NO_2 + h\nu(\lambda < 420\,\text{nm}) \rightarrow NO + O \quad \text{(R1)}$$

This reaction accounts for most of the ozone in the lower atmosphere, as it is followed by

$$O + O_2 + M \rightarrow O_3 + M. \quad \text{(R2)}$$

The photolysis frequency, J, is given by

$$J = \int F(\lambda)\sigma(\lambda)\phi(\lambda)\,\mathrm{d}\lambda \quad (1)$$

where $F(\lambda)$ is the spectral actinic flux (AF) at wavelength λ, $\sigma(\lambda)$ is the absorption cross section of the target molecule, and $\phi(\lambda)$ is the quantum yield of specific photo-products. The spectral actinic flux is defined as the number of photons incident on a sphere, per unit time and wavelength, per unit cross-sectional area of the sphere, i.e., integrating radiation from all directions with equal weight,

$$F(\lambda) = \iint L(\lambda,\theta,\varphi)\sin\theta\, d\theta\, d\varphi \quad (2)$$

where $L(\lambda,\theta,\varphi)$ is the spectral radiance from angular directions θ,φ (Madronich, 1987). The direct solar beam can be a large component of the AF, but diffuse radiation is always important due to the large cross sections for molecular (Rayleigh) scattering at UV wavelengths, scattering by aerosols and clouds, and reflections from the ground.

Aerosols usually attenuate UV radiation reaching the surface, resulting in lower actinic fluxes and photolysis frequencies (Leighton, 1961; Demerjian et al., 1980; Lefer et al., 2003; Flynn et al., 2010; Li et al., 2011). Other pollutants, such as NO_2, may also reduce the actinic flux through direct absorption. However, aerosols in the planetary boundary layer (PBL) also back-scatter incident solar radiation and effectively increase photolysis frequencies above the PBL. Within the PBL, the situation is more complex as aerosols can increase or decrease actinic fluxes, depending on the precise height and aerosol optical properties. For example, Dickerson et al. (1997) found that for the Eastern US, sulfate aerosols, which primarily scatter UV wavelengths, cause an overall increase in PBL actinic fluxes and thus increase regional O_3 by 10–20 ppb. However, Castro et al. (2001) reached the opposite conclusion for Mexico City, where UV-absorbing aerosols reduce PBL actinic fluxes, slowing photochemistry and reducing O_3 maxima by 20–50 ppb. Such changes in O_3 due to aerosol-induced UV perturbations are comparable to or larger than O_3 reductions currently practical with VOC and NO_x emission regulations. The aerosol-induced AF perturbations have been characterized by many modeling studies under different conditions (e.g., Michelangeli et al., 1992; He and Carmichael, 1999; Jacobson, 1998; Liao et al., 1999; Yang and Levy, 2004) and have been parameterized in chemistry-transport models such as WRF-Chem (Grell et al., 2005), CMAQ (Byun and Ching, 1999), CAMx (ENVIRON, 2010), and MOZART (Tie et al., 2005). Quantitative comparisons between measured and simulated AF in the presence of aerosols are fewer, but generally show good agreement from ground stations (Früh et al., 2003) and from aircraft (Kelley et al., 1995; Volz-Thomas et al. 1996; Meloni et al., 2003), although discrepancies at high dust loading were also noted (Junkermann et al., 2002). No detailed comparisons of observed and modeled AF are available for highly polluted urban conditions.

Here, we report measurements of spectral actinic fluxes made at a surface station (T1) on the northern edge of Mexico City during the March 2006 MILAGRO field campaign (Molina et al., 2010), as well as measurements made from the NSF/NCAR C-130 aircraft during several overpasses of the T1 site. A radiative transfer model is used to estimate the relative contributions of NO_2 and aerosols, and to characterize the vertical structure of the UV perturbations. Section 2 describes instruments and measurements used in this work. Section 3 describes the radiative transfer model and Sect. 4 the discussion and results. Conclusions are given in Sect. 5.

2 Measurements

Surface measurements were made during March 2006 at the T1 supersite (Universidad Tecnológica de Tecámac, State of Mexico) of the MILAGRO field campaign. This site is located near the northern edge of Mexico City, at 19.70° N, 98.98° W, 2270 m a.s.l. Measurements at this site are expected to represent a mixture of episodes of cleaner background air, fresh emissions, and intensely polluted plumes immediately downwind of the city. The measurements used in this study are from cloudless days (5, 6, 7, 12, and 13 March) which were identified by visual inspection of radiation measurements and all-sky images. Radiosonde, profiler, and lidar measurements were used by Shaw et al. (2007) to determine the evolution of the boundary layer height (see Fig. 1a) as it grows from a nominal overnight value of a few tens of meters to well over 3000 m by mid-afternoon.

The minimum, maximum, and average NO_2 concentrations used in this work are shown in Fig. 1b. They were

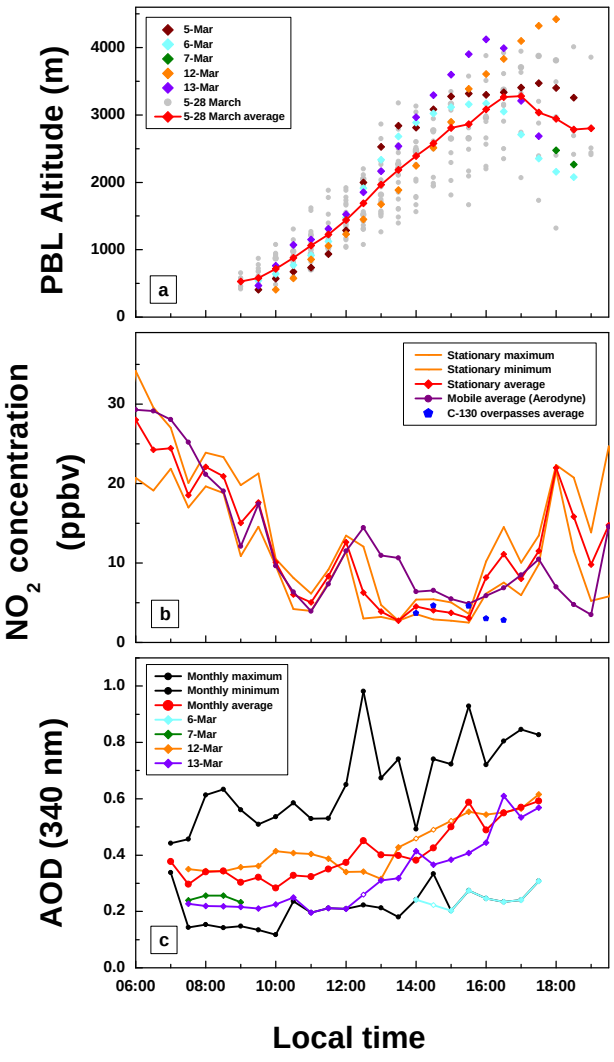

Fig. 1. Diurnal variation at T1 site of **(a)** PBL altitude above ground level (a.g.l.) (color symbols correspond to the cloudless days); **(b)** NO_2 concentration measured by a stationary instrument (6–31 March), a co-located Aerodyne mobile laboratory (19–22 March), and from the C-130 aircraft overpasses (8, 10, 18, 22, and 29 March); **(c)** aerosol optical depth at 340 nm (AERONET, 6–31 March) (open symbols correspond to interpolations).

measured at the T1 site by Laser Induced Fluorescence and corrected for 6 % additional NO_2 fluorescence quenching by H_2O. The minimum and maximum measured values were 1.4 and 65.1 parts per billion by volume (ppbv), respectively. A detailed description of the instrument and technique for LIF detection of NO_2 was given by Day et al. (2002) and Thornton et al. (2000). Measurements of NO_2 at T1 were made on 14 different days (16 to 30 March), although not for the cloudless days used in this work. Thus, 30-min averages were calculated along each day and the half-hour averages of all days were used to create one average NO_2 diurnal profile, which was used as model input. Additional NO_2 measurements, shown in Fig. 1b, were obtained by two other instruments. The first one was a dual-laser Aerodyne Tunable Infrared Laser Differential Absorption Spectrometer (TILDAS) with estimated uncertainty of 8 % (Kolb et al., 2004; Herndon et al., 2007; Dunlea et al., 2007; Wood et al., 2009) deployed 19–22 March at T1 from the Aerodyne Mobile Laboratory. The second instrument was the NCAR 4-channel chemiluminescence instrument mounted aboard the C-130 aircraft. In this case NO_2 was measured as NO following photolytic conversion of NO_2, with a time response of about 3 s due to the residence time in the photolysis cell. The overall estimated uncertainty of the 1-σ values for NO_2 is $\pm(15 + 10\,\%$ of the mixing ratio) pptv (DeCarlo et al., 2008).

The C-130 aircraft flew over the T1 site for a few minutes on 8, 10, 18, 22, and 29 March 2006 during mid to late afternoon local time. An overpass was defined when the C-130 was less than 10 km from T1. For these overpasses the minimum, maximum, and average aircraft heights were 0.5 km, 2.7 km, and 1.6 km above ground level (a.g.l.), respectively. The PBL depths on these days were individually assessed to assure that the flying altitudes during the overpasses were well within this layer. No systematic trend of NO_2 concentrations with altitude (within the PBL) was observed, and horizontal variability was large even during the short overpass times, suggesting the importance of local sources or short-range transport.

Aerosol optical properties were obtained from the AErosol RObotic NETwork (AERONET, Holben et al., 2001) station deployed at the T1 site during the campaign (T1_MAX_MEX, http://aeronet.gsfc.nasa.gov). A CIMEL Electronique 318N sunphotometer measured direct sun radiance every 15 min at 340, 380, 440, 500, 675, 870, and 1020 nm. We used aerosol optical depth at 340 nm (AOD340), single scattering albedo (SSA441) at 441 nm (the shortest wavelength for which SSA retrievals are available), the asymmetry factor (g441) at 441 nm, and the Ångström coefficient (α, 340–440 nm). The AOD340, g441, and α values used in this work are level 2.0, which means that the quality of the data is assured through pre and post field calibrations, automatic cloud clearing, and manual inspection. As no level 2.0 data were available for SSA441, we used level 1.5 values (cloud-screened) for this parameter. No aerosol data were available for 5 March and therefore we used monthly averages for this day. These averages were obtained using all the days for which aerosol data was available in the period 6–31 March. Figure 1c shows the hourly variation of the AOD340 for 6, 7, 12, and 13 March together with the minimum, maximum, and monthly averaged values. Open symbols show interpolations. Because of the nature of the data collection method for almucantar retrievals (SZA $\geq 50°$) and the version 2.0 constraints to assure the data quality, daily observations for g441, SSA441, and α were sparse. Thus, for these parameters the daily averages of the available data were used for the corresponding day.

Actinic flux was measured with three NCAR Scanning Actinic Flux Spectroradiometers (SAFS). One was deployed on the ground at T1 while two were mounted on the C-130 aircraft in order to measure the upwelling and downwelling actinic fluxes aloft. Time synchronization hardware and software assured simultaneous readings at each wavelength. A complete description of the instruments, calibration procedures and installation on the aircraft is given by Shetter and Müller (1999) and Shetter et al. (2003). Briefly, each SAFS collects radiation between 282 and 422 nm from one hemisphere (2π sr). The monochromator was stepped in 1 nm intervals and the acquisition time for each spectrum was about 9 s. The gratings have a ruling of 2400 lines/mm and the entrance and the exit slit widths are fixed to 0.6 mm, resulting in a bandpass (FWHM) of 1.0 nm. Wavelengths between 282 and 288 nm were used to estimate the electronic noise background on a scan by scan basis, since no photons with wavelengths shorter than 290 nm penetrate the atmosphere to the altitude range used in this campaign. In addition, the signal from these wavelengths was used to determine the stray light contribution from visible wavelengths, and apply this correction to all wavelengths. The accuracy of the measurements is estimated to be 6 % in the UV-B and 5 % in the visible (including drift during the campaign) while the optical angular responses of the instruments are ± 3 % for solar zenith angles less than 80°.

Total and diffuse spectral irradiances were measured at the T1 site using United States Department of Agriculture (USDA) UV-B Monitoring Program UV-Multifilter Rotating Shadowband Radiometers (UV-MFRSR) (http://uvb.nrel.colostate.edu/UVB/index.jsf, Bigelow et al., 1998). Direct irradiances were computed by subtracting total and diffuse measurements. Measured voltages were converted to irradiance using the Langley calibration method as described in Corr et al. (2009) for the seven UV wavelengths of the UV-MFRSR (2 nm FWHM): 300, 305, 311, 317, 325, 332, and 368 nm.

3 Radiative transfer model

Simulations of the ultraviolet radiation field were done with the TUV model v.5 (Madronich, 1987; Madronich and Flocke, 1998), for cloudless conditions. The model uses the extraterrestrial solar spectral irradiance (200–1000 nm by 0.01 nm steps, Chance and Kurucz, 2010) and computes its propagation through the atmosphere taking into account multiple scattering and the absorption and scattering due to gases and particles. Both Rayleigh and Mie scattering are considered. The atmosphere was divided in 500 equally spaced 10 m layers up to 5 km a.g.l. to allow high vertical resolution within the PBL, and in 73 equally spaced 1 km layers from 5 km to 78 km a.g.l. All layers have homogeneous composition, temperature, and pressure according to the United States Standard Atmosphere (NOAA, NASA, USAF, 1976). A 4-stream discrete ordinate method (Stamnes et al., 1988) was used and a pseudo-spherical correction was applied to account for Earth's curvature (Petropavlovskikh, 1995). The calculations were carried out at each wavelength from 330 to 420 nm with a resolution of 1 nm to match exactly the resolution of the SAFS instruments. Wavelengths shorter than 330 nm were not considered to avoid possible uncertainties introduced by the total O_3 column values, and to better isolate the effects of NO_2 and aerosols on actinic fluxes. In this way, an uncertainty of ± 25 % in the ozone column only introduces an error less than ± 0.5 % in the actinic flux calculations. Total ozone column values were taken from TOMS satellite archives (http://jwocky.gsfc.nasa.gov) and then, the USSA O_3 profile was scaled to the TOMS values. The actinic flux integrated over 330–420 nm is essentially proportional to the NO_2 photolysis coefficient, but less sensitive to the temperature-dependent NO_2 quantum yield and cross sections, with a ratio of J_{NO_2} to the AF of $(3.80 \pm 0.05) \times 10^{-19}$ cm^2 using the NO_2 spectral data at 273 K from Sander et al. (2011).

Aerosol optical parameters SSA and g were considered wavelength independent. The surface albedo was assumed to be Lambertian and wavelength dependent. Based on the values used in the work of Corr et al. (2009) (which, in turn, is based on the works of Madronich et al., 2007 and Coddington et al., 2008) we used a linear variation of surface albedo from 0.024 at 330 nm to 0.085 at 400 nm. For wavelengths larger than 400 nm a constant value equal to 0.085 was used. The molecular absorption cross section of NO_2 was taken from the JPL 2011 recommendations (Sander et al., 2011).

The model considers both NO_2 and aerosols as well mixed in the PBL and negligible above it. Tethered balloon observations at the T1 site support the first approximation, since they show uniform vertical profiles of ozone and particles from surface up to 700 m a.g.l. (Greenberg et al., 2009). The second approximation is probably less valid because significant amounts of aerosols could be present in the residual layers and free troposphere above the PBL, as seen on 9 March 2006 (see Fig. 3 of Shaw et al., 2007). The large optical depths observed in the morning (Fig. 1c), when the PBL is still rather shallow, also suggest a role for aerosols aloft. While the model can handle arbitrary vertical distributions of pollutants, our choice to limit these to the PBL is for simplicity of interpretation, and recognizing that the more relevant vertical coordinate is optical depth rather than geometric altitude. For aircraft-based measurements, a critical uncertainty is the optical depth remaining above the aircraft, compared to the total measured from the surface by AERONET.

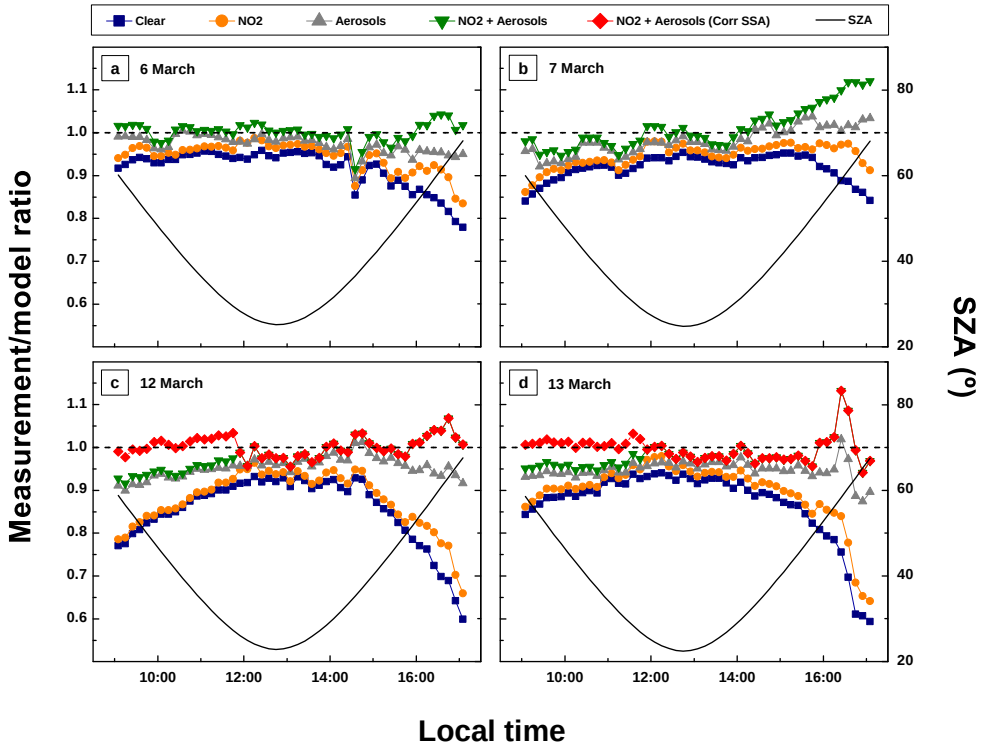

Fig. 2. Actinic flux ratios (measurement/model) for four cloudless days. Symbols and colors correspond to different conditions used for the calculations. Dashed horizontal line corresponds to measurement/model ratio equal to 1.

4 Results and discussion

4.1 Actinic flux at surface

Figure 2 shows the ratios between the actinic flux observations and model calculations at the surface for four cloudless days. Different calculations are shown for clear-sky conditions, and for polluted cases including only NO_2, only aerosols, and both NO_2 and aerosols. For the latter case, we show results using the SSA441, as well as the ultraviolet SSA estimated by Corr et al. (2009) for the morning measurements (see below for additional discussion of the SSA). The clear-sky model overestimates observations by up to 25 % early in the morning, 10 % at noon and 40 % late in the afternoon. Absorption by NO_2 typically accounts for about one quarter of these differences, but can become more significant in the afternoon hours (after 16:30 when the PBL height reaches or is very close to its maximum) accounting occasionally for up to 77 % of the observed differences. This is because, although the NO_2 concentrations at 16:30 LT are similar to those in the morning (around 09:00 LT), the PBL height is between 4 and 9 times higher, as is therefore the column of NO_2. The concentrations of NO_2 reach daytime maxima of 10–15 ppb (see Fig. 1) near noon, and the corresponding reductions in UV radiation are also discernible in Fig. 2.

Figure 3 shows the differences in daily-integrated actinic fluxes between observations and model calculations and also summarizes the relative contributions of NO_2 and aerosols to these differences for each analyzed day. Aerosols account for the larger portion (about three quarters) of the effect of pollutants on the UV radiation field. With their inclusion in the model, agreements with observations are consistently better than ± 10 % in the morning and in the afternoon, improving to ± 3 % at noon. Absorption by NO_2 reduces the actinic flux by about 30 %, several times smaller than the reduction caused by aerosols. Generally, the effect of the NO_2 and aerosols together is slightly larger than the sum of the individual effects. The simple sum explains on average 92 % of the observed differences, while when both are included in the model they account for 95 %. This is because aerosol scattering increases the path length of the photons and therefore the probability to be absorbed by the NO_2. The remaining unexplained percentages (other contributions) are attributed to many factors such as the inherent model and experimental uncertainties, the usage of the SSA at 441 nm, the absence of a diurnal trend in the used SSA values, the usage of average NO_2 concentrations, the assumption of a well-mixed PBL, etc. Still, note that the largest of these unexplained percentages (18.5 % on 13 March) actually represents only a 2.2 % difference between measurements and model calculations.

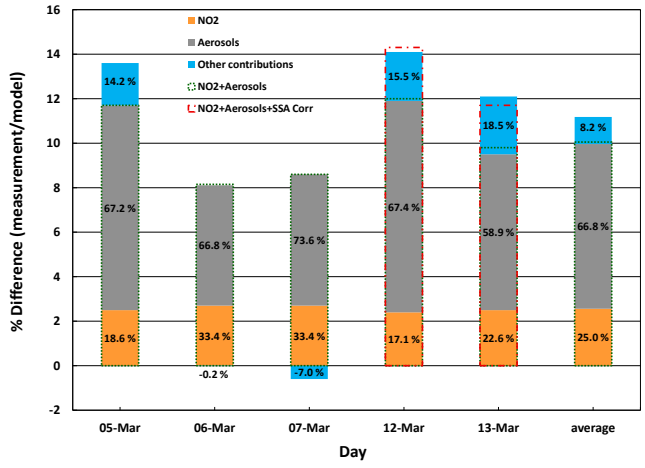

Fig. 3. Percentage difference between observations and clear-sky model calculations of the daily-integrated actinic flux. Different colors correspond to the contribution of NO_2, aerosols, and other sources to these differences. Dotted (green) lines show the effect of including both NO_2 and aerosols in the model. Dashed lines (red) show the results when SSA is corrected.

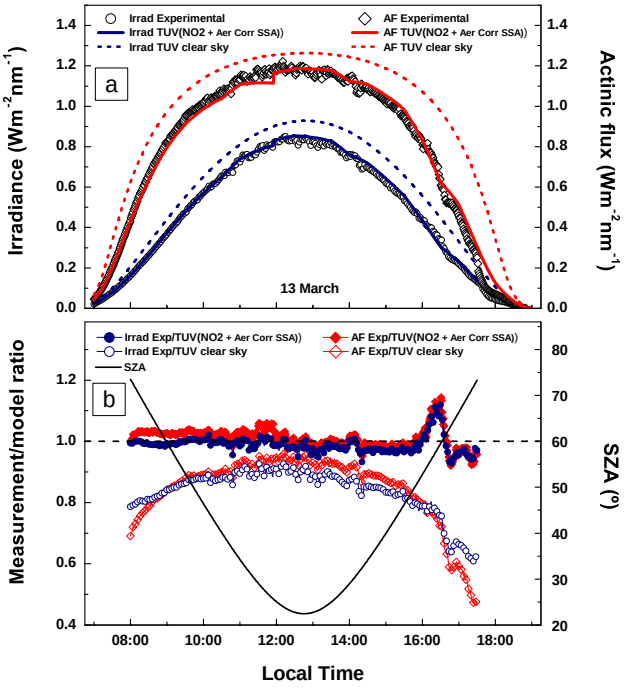

Fig. 4. (a) Daily course of the irradiance and actinic flux at 368 nm for 13 March: measurements and model calculations (clear-sky and polluted). **(b)** The corresponding measurement/model ratios and the solar zenith angle (SZA) variation during this day. Dashed horizontal line corresponds to measurement/model ratio equal to 1.

Despite the good overall agreement, the measured/modeled ratios (Fig. 2) show some residual deviations from unity and some trends through the day (e.g. lower values in the morning of 7 and 12 March). These discrepancies appear to be related to our use in the model of the aerosol SSA determined at 441 nm from AERONET (0.89, 0.86, 0.86, 0.89, and 0.89 for 5, 6, 7, 12, and 13 March, respectively). Considerably lower UV-specific values of the SSA at T1 were recently reported by Corr et al. (2009) for 12 March (0.75–0.83 at 368 nm and 0.78–0.82 at 332 nm) and 13 March 2006 (0.73–0.79 at 368 nm and 0.74–0.78 at 332 nm). A lower value of the SSA for UV wavelengths was also suggested by Barnard et al. (2008) based on spectral irradiance measurements made in Mexico City in 2006. Furthermore, Paredes-Miranda et al. (2009) showed that minimum SSA values (at 532 nm) are found in the early morning and increased markedly until the early afternoon, possibly due to the condensation of secondary organic materials on light-absorbing soot particles. To explore the effect of these uncertainties, we performed simulations using average UV SSAs values from Corr et al. (2009) for the morning hours of 12 March (0.80) and 13 March (0.76). As seen in Figs. 2 and 3, the use of the lower UV SSA gives additional improvement in the comparisons between model and morning observations.

4.2 Irradiance at surface

Actinic flux is the radiative quantity needed to calculate photolysis frequencies, although the irradiance incident on a horizontal surface is the quantity most often measured. Thus, we also examined the effects of NO_2 and aerosols on irradiance. Figure 4a shows the daily course of the measured (UV-MFRSR) and calculated (clear-sky and polluted) spectral irradiance at the surface at 368 nm for 13 March 2006. Calculations before noon were carried out using the Corr et al. (2009) SSA value (0.76, specific for this day and wavelength) while calculations in the afternoon were carried out by using the AERONET SSA441 value (0.89). Spectral AF measurements and calculations at 368 nm are also included in the figure, and were converted to $W\,m^{-2}\,nm^{-1}$ for easier comparison to the irradiance. Note that the absolute value of the AF is larger (by about a factor of 2 for SZA $= 60°$ in accord with simple theory, e.g. Madronich, 1987) because, contrary to the irradiance, it is not weighted by the cosine of the angle of incidence. Figure 4b shows the corresponding ratios between measurements and calculations, together with the SZA variation through the day. The agreement is generally better for irradiance than actinic flux, since the cosine-weighting of the former makes it less sensitive to lateral radiation that can be difficult to fully characterize. Note that at low sun (large SZA), aerosols have a much larger impact (attenuation) on actinic flux than on irradiance. When aerosols and NO_2 are included in the model, both irradiance and actinic flux show much better agreement with measurements. Quantitatively, the daily averaged ratio goes from 0.8 ± 0.1 (clear-sky) to 0.98 ± 0.05 (polluted) for actinic flux and from 0.84 ± 0.07 (clear-sky) to 0.98 ± 0.03 (polluted) for

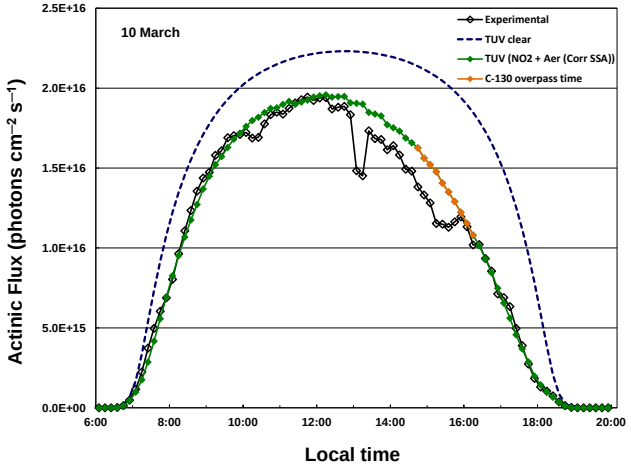

Fig. 5. Daily course of the actinic flux at surface for 10 March 2006. Measurements, calculations for clear sky, and calculations for polluted (NO_2+ aerosols (Corr SSA)) conditions. Orange diamonds show the period in which the C-130 aircraft flew over T1.

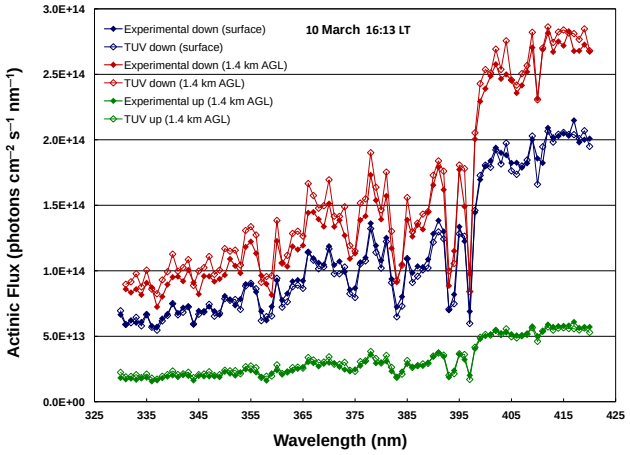

Fig. 6. Spectral variation of the measured and calculated actinic flux at surface and at 1.4 km (a.g.l.) (downwelling and upwelling) for 10 March 2006 at 16:13 local time. PBL altitude at this moment was 3 km (a.g.l.).

irradiance. We again conclude that the lower SSA reported by Corr et al. (2009), about 0.7–0.8, results in better agreement between model and observations of both irradiance and actinic flux in the morning hours.

4.3 Vertical dependence of actinic flux

Overpasses of the T1 site by the C-130 aircraft allow for comparison of actinic fluxes measured simultaneously at the surface and aloft. Figure 5 shows the daily course of the integrated actinic flux at the surface for one overpass day, 10 March 2006. Orange diamonds show the period in which C-130 flew for a few minutes over T1. As in the previous calculations, the AERONET SSA (0.84) was used during the afternoon and a lower one (0.80) during the morning. This figure shows the large effect of the aerosols and NO_2 during this day and also the good agreement between model and measurements at the surface. The asymmetry observed between morning and afternoon values is simulated well by the model, and is attributed to the afternoon increase in the optical columns of aerosol and NO_2. Reductions observed in the periods 10:00–11:30 LT and 12:30–16:00 LT are due to clouds (mostly cirrus clouds, as observed in the sky camera at surface and aircraft cameras). Figure 6 shows spectral actinic fluxes at the T1 surface site and also at an altitude of 1.4 km a.g.l. (downwelling and upwelling) during a C-130 overpass. The good agreement (0.96 ± 0.08) in the upwelling actinic flux over the entire spectral range supports the selected wavelength variation for the model's surface albedo. For the downwelling actinic flux the average spectral agreement at this time was 1.03 ± 0.04 at surface and 1.0 ± 0.2 from the C-130. Note the strong reduction observed in the downwelling actinic flux over an altitude difference of only 1.4 km. A shift in wavelength registration, by about one nm, was evident in the upward-facing aircraft SAFS instrument (downwelling radiation) compared to the other two instruments and the TUV model. This shift was corrected before processing the average spectral agreement. Integrated over 330–420 nm, errors introduced by this shift are minor.

Figure 7 shows the upwelling, downwelling, and total actinic flux ratios between aircraft observations and model calculations for a brief period during the overpass of 10 March. Results for both clear-sky and polluted (NO_2+ aerosols (SSA = 0.84)) model calculations are shown. PBL and aircraft altitudes at these times were 3 km and 1.4 km, respectively. The ratio of observations to clear-sky model for upwelling, downwelling, and total actinic flux is 1.04 ± 0.03, 0.72 ± 0.01, and 0.75 ± 0.01, respectively. When NO_2 and aerosols are included the ratios improve to 0.96 ± 0.03, 0.96 ± 0.02, and 0.96 ± 0.01, respectively. Including all the measurements for this day (54 points) the agreements for the upwelling, downwelling, and total actinic fluxes are 0.99 ± 0.06, 0.94 ± 0.06, and 0.96 ± 0.04, respectively. These results show the model ability to predict the actinic flux in altitude under polluted conditions. They also support the previous assumption of a well-mixed PBL and the use of surface measurements of NO_2 and aerosols as model inputs.

The vertical structure of the AF can become increasingly complex in the presence of aerosols, and while the aircraft measurements do provide some indications, a more complete picture is provided by the model. Figure 8a–c show the variation of the ratios of polluted (only aerosols) to clear-sky actinic flux calculated for 10, 18, and 29 March 2006 at all altitudes below 6 km (a.g.l.) (SSA = 0.8). The color code shows the reductions (blue) and enhancements (red) produced by aerosols as predicted by the model. The C-130 overpass observations are represented by circles at flight altitude, while surface measurements are shown by triangles (both colored

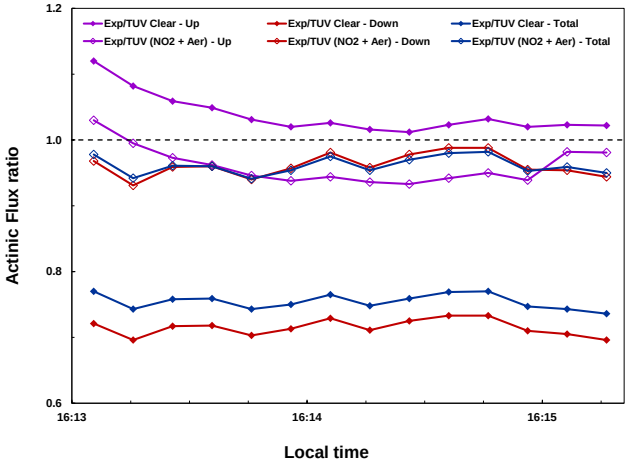

Fig. 7. Upwelling, downwelling, and total actinic flux ratios between the aircraft measurements and model calculations (clear sky and polluted) for 10 March. During this period aircraft altitude was 1.4 km (a.g.l.) and PBL altitude 3 km (a.g.l.). Dashed horizontal line corresponds to measurement/model ratio equal to 1.

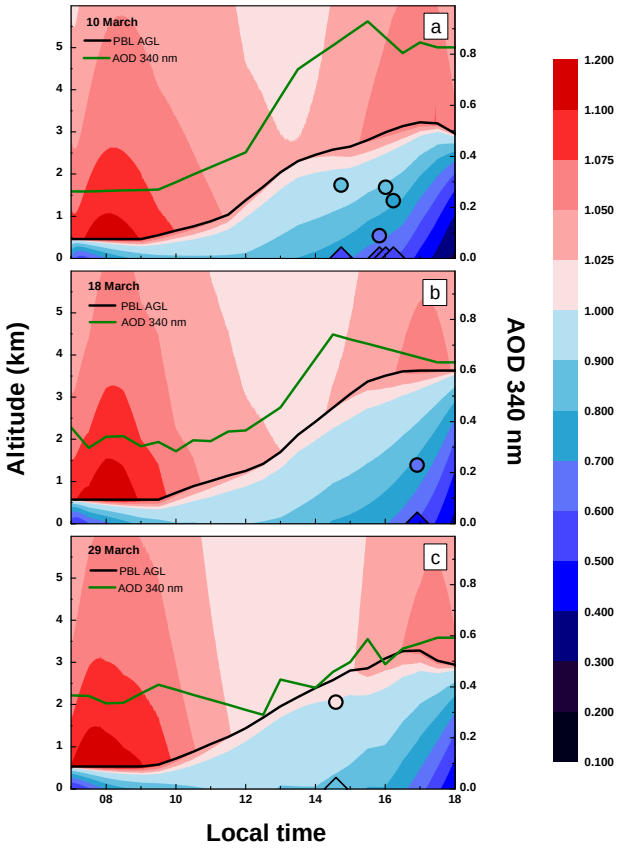

Fig. 8. Hourly variation of the ratios between polluted (only aerosols) and clear-sky total actinic flux model calculations for 10, 18, and 29 March 2006 at all altitudes below 6 km (a.g.l.). Circles represent ratios between C-130 observations and clear-sky model calculations. Triangles represent ratios between surface observations and clear-sky model calculations. Red tones show enhancements while blue tones show reductions with respect to clear-sky AF.

according to their ratio to clear-sky TUV). Figure 8 shows that, compared to clear-sky conditions, actinic fluxes are suppressed in the lower part of the PBL, but are enhanced above it. The enhancements persist into the upper troposphere, and range from a few percent during high sun hours, to more than 20 % just above the shallow morning inversion layer. Surface radiation in the midday is reduced by 10–20 %, but reductions can reach 40–60 % at low sun conditions. Observations, both from C-130 and surface, suggest slightly stronger reductions (as also expected from Fig. 7), but are generally in agreement within 10 % (one color step in the figure).

The apparently complex effects of aerosols on the diurnal and vertical distribution of actinic flux, seen in Fig. 8, can be explained by sensitivity studies with the model, summarized in Fig. 9. The model held constant either the AOD and the PBL height, only the PBL height, or only the AOD (panels a, b, and c, respectively). Absorption by NO_2 was neglected. Figure 9a shows that the relative effect of aerosols is greatest at low sun, for both reduction in the PBL and enhancement above it. This is consistent with a basic property of radiation which states that the reflectivity of a medium (be it aerosol or cloud) increases with the angle of incidence. The diurnal increase in AOD (panel b) leads to larger effects in the afternoon than in the morning. If diurnal growth of the PBL is allowed (panel c) with constant AOD, the pattern of enhancements and reductions follows the PBL height, being more compressed in the morning and stretched vertically in the afternoon. The combined effect of the diurnal cycle of solar zenith angle, PBL height, and aerosol AOD is shown in Fig. 9e, and is essentially identical to the results for the overpass on 10 March shown in Fig. 8a.

Finally, we wish to emphasize the importance of accurate determinations of the SSA by contrasting actinic flux distributions in which the SSA was changed from its model value of 0.8 (panel e) to either 0.6 or 0.95 (panels d and f, respectively). At the lower value (panel d), reductions are seen not only in the PBL but at all altitudes above it, because the absorption by aerosol reduces actinic fluxes up-scattered from the PBL or reflected from the ground. In contrast, a higher SSA (0.95, panel f) enhances actinic fluxes not only above the PBL, but also well below its top, and in some cases almost all the way to the surface. Thus, what may be perceived from surface-based measurements as a reduction may actually be an enhancement when integrated over the entire PBL.

5 Summary and concluding remarks

Actinic fluxes over the wavelength range 330–420 nm measured during MILAGRO were compared with TUV model calculations. Relative to model results for hypothetical

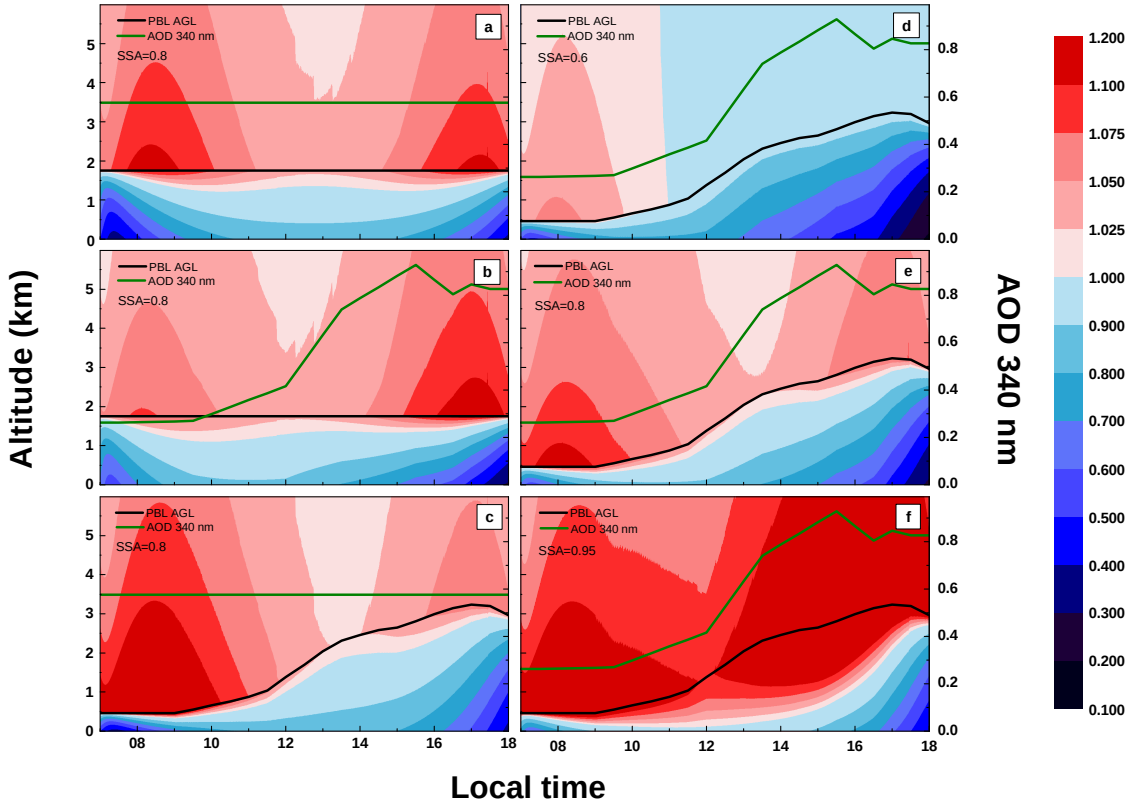

Fig. 9. Hourly variation of the ratios between polluted (only aerosols) and clear-sky total actinic flux model calculations for 10 March 2006 at all altitudes below 6 km (a.g.l.). **(a)** Constant AOD340 and PBL altitude; **(b)** constant PBL altitude; **(c)** constant AOD340; **(d)** SSA = 0.6; **(e)** SSA = 0.8; **(f)** SSA = 0.95.

pollution-free (clear-sky) conditions, measurements show reductions in surface actinic fluxes of 25 % in the morning, 10 % at noon and 40 % in the afternoon. When measured aerosol optical properties and NO_2 concentrations are used as inputs to the model, the reductions are simulated quite well, with average residual discrepancies of less than 5 %. For irradiance measurements at the surface (368 nm) the daily average measurement/model ratio (13 March) was 0.98 ± 0.03. The agreement is better when the lower SSAs measured by Corr et al. (2009) are used rather than the 441 nm AERONET value, at least during the morning. These levels of agreement are comparable to those found in previous studies (e.g., Volz-Thomas et al., 1996; Balis et al., 2002; Früh et al., 2003; Meloni et al., 2003; Palancar et al., 2011) under less polluted conditions, and are remarkable considering the number of assumptions used in the model, particularly regarding aerosol optical depth, single scattering albedo and asymmetry factor, all of which are complex functions of wavelength, temperature, humidity, and other state variables. The ability to predict cloud-free AF with better than 5 % accuracy when aerosol optical properties are reasonably well known means that, in these cases, the uncertainties in photolysis frequencies are dominated by uncertainties in molecular spectra and quantum yields (e.g., Sander et al., 2011) rather than knowledge of the radiation field.

Specifically for Mexico City, Castro et al. (1997, 2001) reported reductions of 20–30 % in actinometrically measured NO_2 photolysis frequencies at urban surface sites in 1994. The smaller effects found here (10–15 % reductions at high sun) stem from both the more suburban location of the T1 site, and a general decrease in aerosol loading over 1994–2006 (Parrish et al., 2011). Li et al. (2011) used the WRF-Chem model to simulate the evolution of aerosol and their effect on photolysis coefficients in the city. Although the absolute agreement with measured actinic fluxes in those simulations was not at the < 5 % accuracy level found here (where observed optical properties were used as input), they find many similar features, e.g. the stronger effects at low sun, and overall reductions in surface ozone of 5–15 %. Taken together, these studies show that the radiative impacts of aerosols and NO_2 are significant and need to be quantified accurately under various real or hypothetical scenarios, as prudent when considering regulations that might alter aerosol optics and so unintentionally influence photochemical ozone production.

The net effect of the photochemistry depends on the actinic flux integrated over the photochemically active volume,

which in this situation is the polluted PBL in the vicinity of Mexico City. As we showed, the altitude dependence here is complex, can be either an overall enhancement or a net reduction, and is very sensitive to the aerosol SSA at wavelengths below 400 nm. Routine measurements (e.g. AERONET) of the SSA are available only at visible wavelengths, and do not accurately represent the SSA at UV wavelengths, which recent studies (Barnard et al., 2008; Marley et al., 2009; Corr et al., 2009) suggest to be considerably lower (more absorptive). In Mexico City, this enhanced absorption at shorter wavelengths may be attributed to absorption by secondary organic aerosols produced in the vigorous photochemical environment of the urban area and/or local sources of strong spectrally absorbing aerosols (e.g. biomass burning). Recent SSA measurements during winter time in Reno, Nevada (39.5° N, 119.8° W) show the opposite trend in that slower photochemical environment, with SSA at UV wavelengths larger (less absorptive) than at visible wavelengths for both polluted and clean days (Gyawali et al., 2012). Better experimental determinations of the SSA at UV wavelengths are needed to provide a more accurate assessment of the vertical distribution, and vertical integral, of the actinic flux within and above the boundary layer.

Acknowledgements. G. G. Palancar would like to thank CONICET for an external fellowship. The National Center for Atmospheric Research is sponsored by the National Science Foundation. We thank AERONET principal investigator Brent Holben and his staff for their efforts in establishing and maintaining the T1_MAX_MEX site. The authors would like to thank R. C. Cohen (University of California, Berkeley) for providing the NO_2 data at surface (LIF) and also to D. J. Knapp, D. D. Montzka, and A. J. Weinheimer (NCAR) for providing the NO_2 measurements taken aboard the C-130 aircraft. Irradiance measurements were provided by the USDA UV-B Monitoring and Research Program supported by USDA/CSREES grant 2006-34263-16326, with additional support from NSF under grant number ATM-0511911.

Edited by: B. Mayer

References

Balis, D. S., Zerefos, C. S., Kourtidis, K., Bais, A. F., Hofzumahaus, A., Kraus, A., Schmitt, R., Blumthaler, M., and Gobbi, G. P.: Measurements and modeling of photolysis rates during the Photochemical Activity and Ultraviolet Radiation (PAUR) II campaign. J. Geophys. Res., 107, 8138, doi:10.1029/2000JD000136, 2002.

Barnard, J. C., Volkamer, R., and Kassianov, E. I.: Estimation of the mass absorption cross section of the organic carbon component of aerosols in the Mexico City Metropolitan Area, Atmos. Chem. Phys., 8, 6665–6679, doi:10.5194/acp-8-6665-2008, 2008.

Bigelow, D. S., Slusser, J. R., Beaubien, A. F., and Gibson, J. H.: The USDA ultraviolet radiation monitoring program, B. Am. Meteorol. Soc., 79, 601–615, 1998.

Byun, D. W. and Ching, J. K. S.: Science algorithms of the EPA Models-3 Community Multiscale Air Quality (CMAQ) modeling system, EPA/600/R-99/030, Off. of Res. and Dev., U.S. Environ. Prot. Agency, Washington, DC, 1999.

Castro, T., Ruiz-Suarez, L. G., Ruiz-Suarez, J. C., Molina, M., and Montero, M.: Sensitivity analysis of an UV radiation transfer model and experimental photolysis rates of NO_2 in the atmosphere of Mexico City, Atmos. Environ., 31, 609–620, 1997.

Castro, T., Madronich, S., Rivale, S., Muhlia, A., andMar, B.: The influence of aerosols on photochemical smog in Mexico City, Atmos. Environ., 35, 1765–1772, 2001.

Chance, K. and Kurucz, R. L.: An improved high-resolution solar reference spectrum for earth's atmosphere measurements in the ultraviolet, visible, and near infrared, J. Quant. Spectrosc. Radiat. Transfer, 111, 9, 1289–1295, doi:10.1016/j.jqsrt.2010.01.036, 2010.

Coddington, O., Schmidt, K. S., Pilewskie, P., Gore, W. J., Bergstrom, R. W., Roman, M., Redemann, J., Russell, P. B., Liu, J., and Schaaf, C. C.: Aircraft measurements of spectral surface albedo and its consistency with ground-based and space-borne observations, J. Geophys. Res., 113, D17209, doi:10.1029/2008JD010089, 2008.

Corr, C. A., Krotkov, N., Madronich, S., Slusser, J. R., Holben, B., Gao, W., Flynn, J., Lefer, B., and Kreidenweis, S. M.: Retrieval of aerosol single scattering albedo at ultraviolet wavelengths at the T1 site during MILAGRO, Atmos. Chem. Phys., 9, 5813–827, doi:10.5194/acp-9-5813-2009, 2009.

Day, D. A., Wooldridge, P. J., Dillon, M. B., Thornton, J. A., and Cohen, R. C.: A thermal dissociation laser-induced fluorescence instrument for in situ detection of NO_2, peroxy nitrates, alkyl nitrates, and HNO_3, J. Geophys. Res., 107, 4046, doi:10.1029/2001JD000779, 2002.

DeCarlo, P. F., Dunlea, E. J., Kimmel, J. R., Aiken, A. C., Sueper, D., Crounse, J., Wennberg, P. O., Emmons, L., Shinozuka, Y., Clarke, A., Zhou, J., Tomlinson, J., Collins, D. R., Knapp, D., Weinheimer, A. J., Montzka, D. D., Campos, T., and Jimenez, J. L.: Fast airborne aerosol size and chemistry measurements above Mexico City and Central Mexico during the MILAGRO campaign, Atmos. Chem. Phys., 8, 4027–4048, doi:10.5194/acp-8-4027-2008, 2008.

Demerjian, K. L., Schere, K. L., and Peterson, J. T.: Theoretical estimates of actinic (spherically integrated) flux and photolytic rate constants of atmospheric species in the lower troposphere, Adv. Environ. Sci. Technol., 10, 369–459, 1980.

Dickerson, R. R., Kondragunta, S., Stenchikov, G., Civerolo, K. L., Doddridge, B. G., and Holben, B. N.: The Impact of Aerosols on Solar Ultraviolet Radiation and Photochemical Smog, Science, 278, 827–830, 1997.

Dimitriades, B.: Effects of hydrocarbon and nitrogen oxides on photochemical smog formation, Environ. Sci. Technol., 6, 253–260, 1972.

Dunlea, E. J., Herndon, S. C., Nelson, D. D., Volkamer, R. M., San Martini, F., Sheehy, P. M., Zahniser, M. S., Shorter, J. H., Wormhoudt, J. C., Lamb, B. K., Allwine, E. J., Gaffney, J. S., Marley, N. A., Grutter, M., Marquez, C., Blanco, S., Cardenas, B., Retama, A., Ramos Villegas, C. R., Kolb, C. E., Molina, L. T., and Molina, M. J.: Evaluation of nitrogen dioxide chemiluminescence monitors in a polluted urban environment, Atmos. Chem. Phys., 7, 2691–2704, doi:10.5194/acp-7-2691-2007, 2007.

ENVIRON: Users Guide: Comprehensive Air quality Model with Extensions (CAMx), Version 5.20, ENVIRON International Corp., Novato, California (www.camx.com), 2010.

Finlayson-Pitts, B. J. and Pitts, J. N.: Chemistry of the Upper and Lower Atmosphere, Academic Press, San Diego, 1999.

Flynn, J., Lefer, B., Rappenglück, B., Leuchner, M., Perna, R., Dibb, J., Ziemba, L., Anderson, C., Stutz, J., Brune, W., Ren, X., Mao, J., Luke, W., Olson, J., Chen, G., and Crawford, J.: Impact of clouds and aerosols on ozone production in Southeast Texas, Atmos. Environ., 44, 4126–4133, 2010.

Früh, B., Eckstein, E., Trautmann, T., Wendisch, M., Fiebig, M., and Feister, U.: Ground-based measured and calculated spectra of actinic flux density and downward UV irradiance in cloudless conditions and their sensitivity to aerosol microphysical properties, J. Geophys. Res., 108, 4509, doi:10.1029/2002JD002933, 2003.

Greenberg, J. P., Guenther, A. B., and Turnipseed, A.: Tethered balloon-based soundings of ozone, aerosols, and solar radiation near Mexico City during MIRAGE-MEX, Atmos. Environ., 43, 2672–2677, 2009.

Grell, G. A., Peckham, S. E., Schmitz, R., McKeen, S. A., Frost, G., Skamarock, W. C., and Eder, B.: Fully coupled "online"chemistry within the WRF model, Atmos. Environ., 39, 6957–6975, 2005.

Gyawali, M., Arnott, W. P., Zaveri, R. A., Song, C., Moosmüller, H., Liu, L., Mishchenko, M. I., Chen, L.-W. A., Green, M. C., Watson, J. G., and Chow, J. C.: Photoacoustic optical properties at UV, VIS, and near IR wavelengths for laboratory generated and winter time ambient urban aerosols, Atmos. Chem. Phys., 12, 2587–2601, doi:10.5194/acp-12-2587-2012, 2012.

Haagen-Smit, A. J., Bradley, C. E., and Fox, M. M.: Ozone formation in photochemical oxidation of organic substances, Ind. Eng. Chem., 45, 2086–2089, 1953.

He, S. and Carmichael, G. R.: Sensitivity of photolysis rates and ozone production in the troposphere to aerosol properties, J. Geophys. Res., 104, 26307–26324, doi:10.1029/1999JD900789, 1999.

Herndon, S. C., Zahniser, M. S., Nelson Jr., D. D., Shorter, J., McManus, J. B., Jiménez, R., Warneke, C., and Gouw, J. A. d.: Airborne measurements of HCHO and HCOOH during the New England Air Quality Study 2004 using a pulsed quantum cascade laser spectrometer, J. Geophys. Res., 112, D10S03, doi:10.1029/2006JD007600, 2007.

Holben, B. N., Tanré, D., Smirnov, A., Eck, T. F., Slutsker, I., Abuhassan, N., Newcomb, W. W., Schafer, J. S., Chatenet, B., Lavenu, F., Kaufman, Y. J., Castle, J. Vande, Setzer, A., Markham, B., Clark, D., Frouin, R., Halthore, R., Karneli, A., O'Neill, N. T., Pietras, C., Pinker, R. T., Voss, K., and Zibordi, G.: An emerging ground-based aerosol climatology: Aerosol Optical depth from AERONET, J. Geophys. Res., 106, 12067–12097, 2001.

Jacobson, M. Z.: Studying the effects of aerosols on vertical photolysis rate coefficient and temperature profiles over an urban airshed, J. Geophys. Res., 103, 10593–10694, 1998.

Junkermann, W., Brühl, C., Perner, D., Eckstein, E., Trautmann, T., Früh, B., Dlugi, R., Gori, T., Ruggaber, A., Reuder, J., Zelger, M., Hofzumahaus, A., Kraus, A., Rohrer, F., Brüning, D., Moortgat, G., Horowitz, A., and Tadic, J.: Actinic radiation and photolysis processes in the lower troposphere: Effect of clouds and aerosols, J. Atmos. Chem., 42, 413–441, 2002.

Kelley, P., Dickerson, R. R., Luke, W. T., and Kok, G. L.: Rate of NO_2 photolysis from the surface to 7.6 km altitude in clear-sky and clouds, Geophys. Res. Lett., 22, 2621–2623, 1995.

Kleinman, L. I.: The dependence of tropospheric ozone production rate on ozone precursors, Atmos. Environ., 39, 575–586, 2005.

Kolb, C. E., Herndon, S. C., McManus, J. B., Shorter, J. H., Zahniser, M. S., Nelson, D. D., Jayne, J. T., Canagaratna, M. R., and Worsnop, D. R.: Mobile Laboratory with Rapid Response Instruments for Real-Time Measurements of Urban and Regional Trace Gas and Particulate Distributions and Emission Source Characteristics, Environ. Sci. Technol., 38, 5694–5703, 2004.

Lefer, B. L., Shetter, R. E., Hall, S. R., Crawford, J. H., and Olson, J. R.: Impact of clouds and aerosols on photolysis frequencies and photochemistry during TRACE-P: 1. Analysis using radiative transfer and photochemical box models, J. Geophys. Res., 108, 8821, doi:10.1029/2002JD003171, 2003.

Leighton, P. A.: Photochemistry of Air Pollution, Academic Press, New York, 13–16, 1961.

Li, G., Bei, N., Tie, X., and Molina, L. T.: Aerosol effects on the photochemistry in Mexico City during MCMA-2006/MILAGRO campaign, Atmos. Chem. Phys., 11, 5169–5182, doi:10.5194/acp-11-5169-2011, 2011.

Liao, H., Yung, Y. L., and Seinfeld, J. H.: Effects of aerosols on tropospheric photolysis rates in clear and cloudy atmospheres, J. Geophys. Res., 104, 23697–23707, 1999.

Madronich, S.: Photodissociation in the atmosphere: 1. Actinic flux and the effect of ground reflections and clouds, J. Geophys. Res., 92, 9740–9752, 1987.

Madronich, S. and Flocke, S.: The role of solar radiation in atmospheric chemistry, in: Handbook of Environmental Chemistry, edited by: Boule, P., Springer-Verlag, Heidelberg, 1–26, 1998.

Madronich, S., Shetter, R., Hall, S., Lefer, B., and Slusser, J.: Ultraviolet characteristics of PBL aerosol in Mexico City, Eos Trans. AGU, 88(52), Fall Meet. Suppl., Abstract A32 A-06, 2007.

Marley, N. A., Gaffney, J. S., Castro, T., Salcido, A., and Frederick, J.: Measurements of aerosol absorption and scattering in the Mexico City Metropolitan Area during the MILAGRO field campaign: a comparison of results from the T0 and T1 sites, Atmos. Chem. Phys., 9, 189–206, doi:10.5194/acp-9-189-2009, 2009.

Meloni, D., di Sarra, A., Fiocco, G., and Junkermann, W.: Tropospheric aerosols in the Mediterranean: 3. Measurements and modeling of actinic radiation profiles, J. Geophys. Res., 108, 4323, doi:10.1029/2002JD003293, 2003.

Michelangeli, D. V., Allen, M., Yung, Y. L., Shia, R. -L, Crisp, D., and Eluszkiewicz, J.: Enhancement of atmospheric radiation by an aerosol layer, J. Geophys. Res., 97, 865–874, 1992.

Molina, L. T., Madronich, S., Gaffney, J. S., Apel, E., de Foy, B., Fast, J., Ferrare, R., Herndon, S., Jimenez, J. L., Lamb, B., Osornio-Vargas, A. R., Russell, P., Schauer, J. J., Stevens, P. S., Volkamer, R., and Zavala, M.: An overview of the MILAGRO 2006 Campaign: Mexico City emissions and their transport and transformation, Atmos. Chem. Phys., 10, 8697–8760, doi:10.5194/acp-10-8697-2010, 2010.

National Oceanic and Atmospheric Administration (NOAA), National Aeronautics and Space Administration (NASA), United States Air Force (USAF): US Standard Atmosphere, Washington, DC, US Government Printing Office, 1976.

Palancar, G. G., Shetter, R. E., Hall, S. R., Toselli, B. M., and Madronich, S.: Ultraviolet actinic flux in clear and cloudy atmospheres: model calculations and aircraft-based measurements, Atmos. Chem. Phys., 11, 5457–5469, doi:10.5194/acp-11-5457-2011, 2011.

Paredes-Miranda, G., Arnott, W. P., Jimenez, J. L., Aiken, A. C., Gaffney, J. S., and Marley, N. A.: Primary and secondary contributions to aerosol light scattering and absorption in Mexico City during the MILAGRO 2006 campaign, Atmos. Chem. Phys., 9, 3721–3730, doi:10.5194/acp-9-3721-2009, 2009.

Parrish, D., Singh, H., Molina, L., and Madronich, S.: Air quality progress in North American megacities: A review, Atmos. Environ., 45, 7015–7025, 2011.

Petropavlovskikh, I.: Evaluation of Photodissociation Coefficient Calculations for Use in Atmospheric Chemical Models, Ph.D. thesis, University of Brussels/ National Center for Atmospheric Research, Cooperative Thesis No. 159, NCAR, Boulder, Colorado, USA, 1995.

Sander, S. P., Abbatt, J., Barker, J. R., Burkholder, J. B., Friedl, R. R., Golden, D. M., Huie, R. E., Kolb, C. E., Kurylo, M. J., Moortgat, G. K., Orkin, V. L., and Wine P. H.: Chemical Kinetics and Photochemical Data for Use in Atmospheric Studies, Evaluation No. 17, JPL Publication 10-6, Jet Propulsion Laboratory, Pasadena, http://jpldataeval.jpl.nasa.gov, 2011.

Shaw, W. J., Pekour, M. S., Coulter, R. L., Martin, T. J., and Walters, J. T.: The daytime mixing layer observed by radiosonde, profiler, and lidar during MILAGRO, Atmos. Chem. Phys. Discuss., 7, 15025–15065, doi:10.5194/acpd-7-15025-2007, 2007.

Shetter, R. E. and Müller, M.: Photolysis frequency measurements using actinic flux spectroradiometry during the PEM-Tropic mission: Instrumentation description and some results, J. Geophys. Res., 104, 5647–5661, 1999.

Shetter, R. E., Cinquini, L., Lefer, B. L., Hall, S. R., and Madronich, S.: Comparison of airborne measured and calculated spectral actinic flux and derived photolysis frequencies during the PEM Tropics B mission, J. Geophys. Res., 108, 8234, doi:10.1029/2001JD001320, 2003.

Sillman, S.: The relation between ozone, NO_x and hydrocarbons in urban and polluted rural environments, Atmos. Environ., 33, 1821–1845, 1999.

Stamnes, K., Tsay, S., Wiscombe, W., and Jayaweera, K.: Numerically stable algorithm for discrete-ordinate-method radiative transfer in multiple scattering and emitting layered media. Appl. Optics, 27, 2502–2509, 1988.

Stephens, S., Madronich, S., Wu, F., Olson, J. B., Ramos, R., Retama, A., and Muñoz, R.: Weekly patterns of México City's surface concentrations of CO, NO_x, PM_{10} and O_3 during 1986–2007, Atmos. Chem. Phys., 8, 5313–5325, doi:10.5194/acp-8-5313-2008, 2008.

Thornton, J. A., Wooldridge, P. J., and Cohen, R. C.: Atmospheric NO_2: In Situ Laser-Induced Fluorescence Detection at Parts per Trillion Mixing Ratios, Anal. Chem., 72, 528–539, 2000.

Tie, X., Madronich, S., Walters, S., Edwards, D., Ginoux, P., Mahowald, N., Zhang, R. Y., Lou, C., and Brasseur, G.: Assessment of the global impact of aerosols on tropospheric oxidants, J. Geophys. Res., 110, D03204, doi:10.1029/2004JD005359, 2005.

Volz-Thomas, A., Lerner, A., Pätz, H. -W., Schultz, M., McKenna, D. S., Schmitt, R., Madronich, S., and Röth, E. P.: Airborne Measurements of the photolysis frequency of NO_2, J. Geophys. Res., 101, 18613–18627, 1996.

Wood, E. C., Herndon, S. C., Onasch, T. B., Kroll, J. H., Canagaratna, M. R., Kolb, C. E., Worsnop, D. R., Neuman, J. A., Seila, R., Zavala, M., and Knighton, W. B.: A case study of ozone production, nitrogen oxides, and the radical budget in Mexico City, Atmos. Chem. Phys., 9, 2499–2516, doi:10.5194/acp-9-2499-2009, 2009.

Yang, H. and Levy II, H.: Sensitivity of photodissociation rate coefficients and O_3 photochemical tendencies to aerosols and clouds, J. Geophys. Res., 109, D24301, doi:10.1029/2004JD005032, 2004.